Nanoscale

PAPER

View Article Online
View Journal | View Issue

Cite this: *Nanoscale*, 2015, **7**, 15895

High temperature continuous flow synthesis of CdSe/CdS/ZnS, CdS/ZnS, and CdSeS/ZnS nanocrystals†

Matt S. Naughton,[a] Vivek Kumar,[a] Yolanda Bonita,[a] Kishori Deshpande[b] and Paul J. A. Kenis*[a]

Received 7th July 2015,
Accepted 24th August 2015

DOI: 10.1039/c5nr04510j

www.rsc.org/nanoscale

Continuous flow reactors show great promise for large-scale synthesis of quantum dots. Here, we discuss results for the synthesis of multi-layered Cd-based hybrid nanocrystals – CdSe/CdS/ZnS, CdS/ZnS, and CdSeS/ZnS – in a continuous flow reactor. The simple reactor design and liquid-phase chemistry obviate the need for preheating or in-line mixing, and the chosen reactor dimensions and operating conditions allow for high flow rates (~10 mL min^{-1}). Additionally, the simple reactor design is well suited for scale-up. The CdSe/CdS/ZnS particles synthesized at elevated temperatures in the reactor exhibit quantum yields of over 60% at longer wavelengths (red region). The shell growth for these particles is conducted without the need for complex dropwise addition or SILAR shell growth procedures used in batch reactors. CdS-based particles were shown to have a higher performance when using octadecene-S instead of TOP-S, which improved the quality of shell growth. In addition, stoichiometric synthesis of the alternate CdSeS/ZnS alloy particles was conducted, removing the need for a large excess of S to offset the lower S reactivity. CdSeS/ZnS alloy nanoparticles exhibit quantum yields of about 50% in the intermediate wavelength range (500–600 nm).

Introduction

Cadmium-based semiconductor nanocrystals have been the subject of intense study for their fluorescent properties.[1,2] These nanocrystals have many applications including solid-state lighting, displays, and fluorescence tagging.[1–3] Traditionally, Cd-based nanocrystals are based around CdSe for emission at green to red wavelengths or CdS for violet-blue emission.[3] Growth of a passivating ZnS shell substantially increases quantum yield for both CdSe and CdS;[3–8] CdSe/CdS/ZnS or CdSe/ZnSe/ZnS particles have the passivating benefits of ZnS combined with lower lattice strain between CdSe and the intermediate layer.[6]

Scalable quantum dot synthesis is hampered by several challenges. Quantum dots are typically synthesized using a hot injection method, where a burst of nucleation from relatively rapid mixing is used to create a large number of nanoparticles. However, this method is difficult to scale into large batches due to mixing issues; in addition, batch reactions have the intrinsic disadvantage of loading and unloading times.[3] Non-injection syntheses (also known as the "heating-up method"[9]), where the reactants are mixed at room temperature and then heated gradually to the target temperature, are more scalable, but still suffer from the general disadvantages of batch reactions. Additionally, batch reactions often employ dropwise addition of Zn for shell growth, which is very difficult to directly translate to a flow reactor.[10] Direct imitation of dropwise addition in a flow reactor would require fast mixing of droplets added at regular residence time intervals, greatly increasing reactor complexity and pressure drop. The alternative shell growth method using successive ion layer adhesion and reaction (SILAR) shows promise, but requires two injections per monolayer[6] which poses reactor design challenges for large shells.

More recently, quantum dot synthesis in microfluidic flow reactors has demonstrated promise for scalable synthesis.[11,12] Microfluidic reactors have the advantage of rapid heating/cooling and offer higher throughput than hot injection batch systems.[3,10,13–15] The addition of high quality microfluidic mixers can offer mixing times of less than a second at the cost of increased pumping losses due to pressure drop. Microfluidic tube reactors using PTFE or steel tubes have been shown to produce quality Cd-based nanocrystals with

[a]*Chemical & Biomolecular Engineering, University of Illinois at Urbana-Champaign, 600 South Mathews Ave, Urbana, IL 61801, USA. E-mail: kenis@illinois.edu*
[b]*The Dow Chemical Company, 2301 North Brazosport Boulevard, Freeport, TX 77541, USA*
†Electronic supplementary information (ESI) available. See DOI: 10.1039/c5nr04510j

quantum yields of up to 78%.[3,10] With a more complex emulsion-based microreactor, CdSe particles with full width at half maximum (FWHM) of 27 nm were successfully generated.[13] Use of a microreactor can also narrow particle size distribution.[16]

However, with limited exceptions, many microreactor synthesis methods are constrained by lower reactant throughput.[14,15] The relatively low volumetric flow rates (on the order of μL min^{-1}) used with these designs limits the mass production rate of the quantum dots.[17] Microreactor channel diameters are in the range of 0.3 mm,[3] which causes high pumping losses and may cause challenges when scaling out to multi-channel configurations for large-scale production. Droplet-based reactors, in addition to addressing mixing issues, show promise in the direction of high throughput production of quantum dots. A recent work by DeMello' group demonstrated the ability to produce substantial amounts of quantum dots on a robust droplet-based continuous reactor (~150 g per day), which is a significant demonstration of micro-reactor viability.[14,15,18] However, droplet-based continuous syntheses are associated with a few challenges – additional separation steps and narrower flow rate ranges for stable droplet formation. Furthermore, the carrier liquid can also affect the course of the reaction; common inert fluorocarbon carrier liquids can contain large amounts of dissolved gases, which may affect the reaction near the droplets' interface.

In this work, we demonstrate a streamlined "heat injection" continuous flow system for core-multishell quantum dot synthesis. This reactor uses liquid-phase chemistry that is not mixing-sensitive at room temperature, eliminating the need for any preheating or in-line mixing, and has channels that are of the order of 1 mm in diameter, thus suitable for rapid heating/cooling. Shell growth is conducted with a single mixing step or even no additional steps, in the case of CdSe/CdS; this methodology eliminates the need for the multiple injections required to simulate dropwise addition. We apply this millifluidic reactor to the known systems of CdSe/CdS/ZnS and CdS/ZnS. In addition, we demonstrate the ability to synthesize CdSeS/ZnS alloy nanoparticles which to our knowledge has not been shown previously in a continuous flow system.

Experimental

Reactor design

The reactor is a stainless steel coil with an inner diameter of 2.2 mm and an outer diameter of 3.2 mm, indicating millifluidic dimensions.[19,20] The total volume was 7.24 ml for the CdSe synthesis or 16.8 ml for the CdS and CdSeS syntheses. With the flow rates used, the Reynolds number is smaller than 200, indicating laminar flow; thus, the mixing of reactants prior to being introduced to the stainless steel reactor is the dominant source of mixing. Inside the reactor, mixing occurs through diffusive mixing. The results between the two reactors were compared by running an identical trial in each reactor and determined to be the same for constant residence times, which is supported by literature.[17] The temperature of the reactor is held constant using an oil bath full of Dynalene HT (Dynalene Inc), which has a boiling point >385 °C that is well above the 270 °C temperature used here. The oil bath was heated using an EchoTherm HP40 hot plate (Torrey Pines Scientific) and the temperature was measured using a stainless steel immersion probe (Torrey Pines Scientific). The reactants were supplied by a PHD 2000 syringe pump (Harvard Apparatus), which was connected to the reactor using PTFE tubing. The effluent from the reactor was collected in open air in glass vials; the length of the outlet tubing ensured that the reactants were cooled below the 250 °C auto ignition temperature of octadecene.

Synthesis chemistry

Cadmium oxide (99.5%), selenium (99.99%), sulfur (99.98%), oleic acid (90%), oleylamine (70%), octadecene (ODE) (90%), trioctylphosphine (TOP) (90%), and zinc diethyldithiocarbamate ($ZnDDTC_2$) (97%) were ordered from Sigma-Aldrich. Unless stated otherwise, the quantum dot synthesis used 0.0663 g CdO (0.51 mmol) dissolved in 3.1 mL of oleic acid at 200 °C forming a clear solution. For CdSe, TOP-Se solution was created by mixing 0.041 g Se with 4.8 mL ODE and 0.34 mL TOP and heating to 100 °C for 10 minutes under nitrogen. For CdS, ODE-S solution was created by mixing 0.0167 g S (0.51 mmol) with 5.1 mL ODE and heating to 70 °C in air. For CdSeS, the anion solution was the same 5.1 mL volume and was composed of 50 vol% TOP-Se solution and 50 vol% ODE-S solution. For a standard synthesis, 3.1 mL of the Cd oleate solution (0.16 M Cd) and 5.1 mL of the anion solution (0.1 M Se or S) was mixed with 51 mL ODE for approximately one minute and pumped through the tube reactor, which was held at 270 °C with standard residence times (reactor volume/volumetric flow rate) of three minutes.

For shell growth, a standard stock solution of 0.058 g $ZnDDTC_2$ dissolved in 1.6 mL of TOP (0.1 M $ZnDDTC_2$) was used. Standard shell addition amounts were 1.6 mL of the $ZnDDTC_2$ solution in TOP mixed with 1.6 mL of oleylamine (as a sacrificial amine for the $ZnDDTC_2$ decomposition) and 10 mL of reacted core solution. The amount of $ZnDDTC_2$ added roughly corresponds to 2 monolayers, which is within the optimal range for CdSe/ZnS.[21] The reactants were mixed and pumped through the tube reactor at 140 °C for five minutes for CdSe; for CdS and CdSeS, an improved shell growth procedure of 110 °C for 30 minutes was used instead. The reactor was flushed with ODE after each run; the flushed ODE did not exhibit fluorescence under UV light, indicating the absence of quantum dots. In addition, a reactor was cut open after being used ~50 runs and showed no apparent buildup. The reactor was cut open at two different places to check for any quantum dot deposition. The images (ESI†) indicate no such deposition.

Characterization

The solutions were typically diluted 1 : 40 in chloroform to obtain absorbance between 0.02 and 0.1 absorbance units

(substantial additional dilution was required for CdS and sometimes for other samples) and were imaged in solution without additional purification or size selection. The purification process involves mixing of the sample with methanol and ethanol in a 5 : 1 alcohol : effluent ratio, shaking to generate an emulsion, centrifuging at 3000 rpm for 5 minutes, decanting the liquid phase, and finally suspending in hexane. Fluorescence results from a common purification process were within 90–110% of the values obtained from the as-synthesized solution.[14] Absorption spectra were obtained from an 8453 UV-Vis Diode Array System spectrophotometer (Agilent) and fluorescence spectra were obtained from a Jobin-Yvon Fluoromax-3 spectro-fluorimeter (Horiba); a 490 nm excitation wavelength was used for CdSe and excitation at 350 nm was used for CdS and CdSeS. Quantum yields (QY) were determined by comparing to a quinine sulfate solution in 0.1 M H_2SO_4 (58% quantum yield).[22] For CdSe, this method had questionable applicability due to the different excitation wavelength; therefore, quantum yield was also determined using a Quantamaster 40 spectrophotometer (Photon Technology International) at the Midland research facility of The Dow Chemical Company, which was found to agree with the value relative to quinine sulfate within 5%.

Results and discussion

Mixing time sensitivity

Among the different operational parameters, we explored the possible effect of mixing time first. For these experiments solutions of the Cd^{2+} cation and Se (or S) precursors where mixed in less than 1 min in a beaker, so offline. Subsequently, the experiment was conducted by using a syringe pump to introduce the mixture into the reactor. Other reactor setups reported in the literature[3] incorporate inline mixing where a Cd stream is mixed with a Se stream at low temperature, then heated in the reactor. For these chemistries, the reactants appear to have minimal sensitivity to mixing time at room temperature; spectra of a Cd + Se reagent mixture left overnight at room temperature yielded no fluorescence or particle formation. Based on this result, mixing could be done on a larger scale over the course of hours, simplifying reactor design and minimizing the need for microscale inline mixers. For the purposes of this study, cold offline mixing appears equivalent to cold inline mixing, allowing for the heat injection setup where the premixed reactants are rapidly heated to the reaction temperature. Other parameters such as time, temperature, and shell thickness were explored in experiments specific to the reactant system.

Synthesis of CdSe nanoparticles

The initial goal for these experiments was to make CdSe nanoparticles using a relatively air-insensitive procedure. Many literature procedures use trioctylphosphine oxide (TOPO) as a solvent, which has the disadvantage of being solid at room temperature, and/or use dimethyl cadmium or hydrogen selenide/sulfide, which are highly toxic gases. Here, we focus on a lower cost and less hazardous CdSe synthesis, using CdO reacted with bioavailable oleic acid and Se reacted with TOP in a solvent primarily composed of ODE. This system is entirely liquid phase, making it suitable for pumping at low temperature. The initial Cd : Se molar ratio was 1.44 with a Cd concentration of 0.008 M.

Initial studies explored the effects of temperature on particle fluorescence. Initial tests were conducted at 220 °C and 270 °C, along with a batch experiment conducted at 180 °C. The highest temperature of 270 °C gave substantially higher fluorescence than the other samples, which is likely due to reduced defects at higher temperature along with greater conversion and is consistent with literature results. The FWHM, which is correlated to the size dispersion of the particles, is 38 nm at 270 °C, 35 nm at 225 °C, or 130 nm at 180 °C (in batch). These FWHMs are relatively wide and indicative of breadth of nanoparticle sizes, which may be due to several process factors. Some possibilities are lower temperature as compared to other procedures, which may be 300 °C or higher, or use of a non-coordinating solvent, since ODE is the bulk of the system and does not act as a capping agent to slow growth. Additionally, using a constant temperature zone instead of higher temperature injection followed by lower temperature growth could also broaden particle size distribution. Broader particle size distribution may also be caused by axial dispersion in the reactor. Based on these trials, 270 °C was used for subsequent experiments due to its higher fluorescence and adequate FWHM.

ZnS shell growth over CdSe

The standard procedure in the literature is to grow a shell, typically ZnS, over the CdSe cores to passivate the particle and thus enhance fluorescence. However, literature methods often use dropwise addition of Zn precursors, which is not possible to simulate in the present reactor and would cause scaling challenges (Fig. 1). An alternate method mentioned in several studies[4,5,10] is to use a single source precursor, zinc diethyldithiocarbamate (Zn $DDTC_2$), which thermally decomposes into ZnS[5] according to eqn (1)–(2):

$$Zn(S_2CNEt_2)_2 + 2NH_2R \rightarrow ZnS + H_2S + 2S{=}C(NEt_2)(NHR) \quad (1)$$

$$S{=}C(NEt_2)(NHR) + NH_2R \rightarrow S{=}C(NHR)_2 + NHEt_2 \quad (2)$$

Use of this precursor allows for premixing of the reactants without any intermediate purification steps, consistent with the core synthesis method and compatible with potential addition of inline mixing. The amount of ZnS precursor added was calculated to be ~2 monolayers based on literature correlations.[21] TOP was used to solubilize and stabilize the $ZnDDTC_2$ to create a 0.1 M concentration of $ZnDDTC_2$ in TOP. Oleylamine was also added as the sacrificial amine in large molar excess at a volumetric ratio of 1.6 ml oleylamine/10 ml core solution; oleylamine may have also acted as a secondary

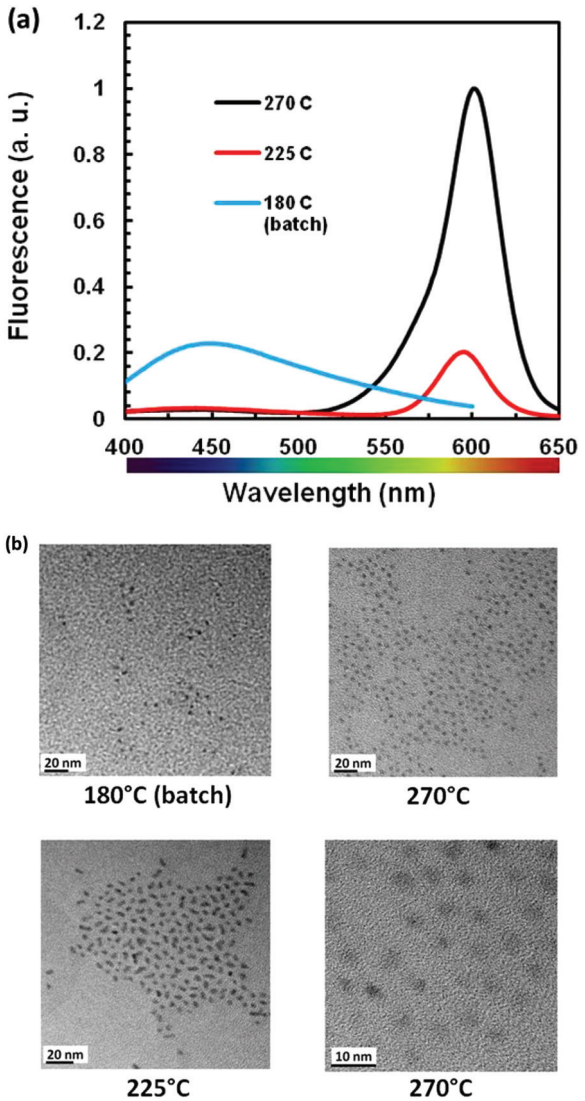

Fig. 1 (a) Fluorescence spectra of CdSe particles synthesized at varying temperatures and (b) corresponding TEM images showing wide particle size distribution for 180 °C and 225 °C. Fluorescence values are normalized where the peak value for 270 °C = 1. Excitation: 350 nm.

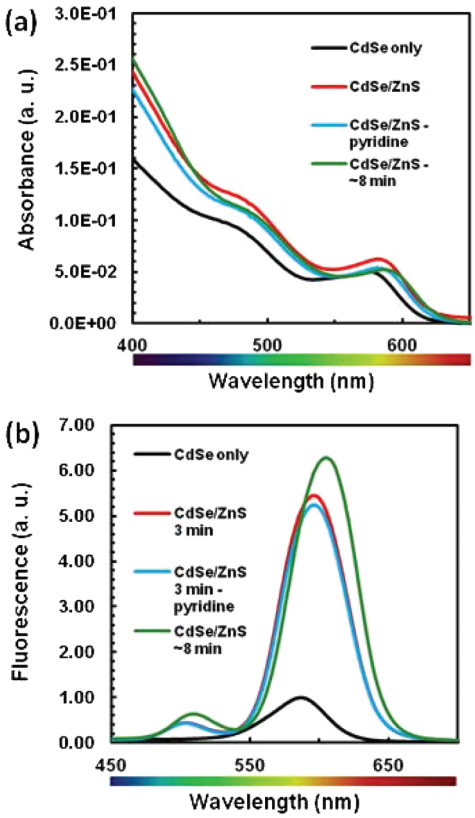

Fig. 2 (a) Absorbance and (b) fluorescence spectra of CdSe/ZnS quantum dots in arbitrary units with varying residence time and pyridine treatment. The pyridine-treated sample was diluted 1 : 1 with pyridine and then diluted to the same concentration as the standard CdSe/ZnS dots.

capping agent. The resulting mixture remained liquid and was straightforward to pump at room temperature.

The resulting CdSe/ZnS quantum dots were substantially more fluorescent than the CdSe cores, as shown in Fig. 2. The absorption of the core–shell particles increased with shell growth by a factor of 1.2; by contrast, the fluorescence of the particles, shown here normalized to the maximum for the core particles, increased by a factor of 5 for a three minute residence time or a factor of 6 for an eight minute residence time. These results show substantial fluorescence improvement for the core–shell particles even when considering the increase in absorption. Another test for the core–shell particle enhancement involved mixing the particles with pyridine in a 1 : 1 volumetric ratio. Pyridine is an alternate ligand that can quench the fluorescence of core particles due to incomplete ligand exchange from mixing at room temperature. Mixing with pyridine quenched CdSe particles synthesized in the flow reactor. The fluorescence results demonstrate minimal quenching from the presence of pyridine, further demonstrating successful shell growth. The FWHM of the particles increased by 5 nm while the peak location red-shifted by 10 nm, from 587 nm to 597 nm, during shell growth.

The quantum yield of the samples was measured *versus* quinine sulfate; an integrated sphere was used to verify that the relative quantum yields obtained were accurately translated into absolute quantum yield. The quantum yield was calculated using the standard method of determining absorbance-normalized fluorescence output relative to the dye, then multiplying by the quantum yield of the quinine sulfate dye (58%). Quinine sulfate was used instead of Rhodamine to enable better comparison with CdS and CdSeS particles. The quantum yield calculated from the results was 2% for the core particles and 12% for the core–shell particles, which is low compared to results reported in the literature.[10,16] In the setup used here, the throughput was 10–15× higher than a similar synthesis conducted in a stainless steel tube reactor.[17] This enhanced throughput can be explained by the use of higher reagent concentrations in this millifluidic reactor. However,

the quantum yield was lower than the 28% reported in the literature, indicating that improved quantum yield was the next goal. To improve performance, the synthesis procedure was changed to use 1 : 1 stoichiometry and a longer shell growth time of five minutes; the quantum yield increased to 20%, but this performance was still relatively low.

Synthesis of CdSe/CdS/ZnS nanoparticles

To further improve the performance of the CdSe particles, an alternate shell was used to minimize lattice strain. CdS has a lattice constant similar to CdSe with a lattice mismatch of only 4% as compared to the ZnS mismatch of 12%; this property demonstrates that CdS can be a shell material that will cause fewer defects and traps from the lattice mismatch.[6,7] Although there are several methods to synthesize a CdS shell (dropwise addition of Cd or S, Cd diethyldithiocarbamate decomposition, SILAR synthesis of CdS layer(s)), a simpler method was tested where TOP-S was used in place of a fraction of the TOP-Se. Since Se has a higher reactivity than S, the CdSe cores nucleate first followed by CdS overgrowth within a single reactor stage. This theory is supported by the fluorescence results in Fig. 3, where the core–shell particles are substantially blue-shifted relative to the core–shell particles using only Se in the initial step. Similar peak locations to the 10 : 90 Se : S particles were obtained with particles using a 10% Se concentration with the same concentration of Cd, indicating the CdSe core has a similar size independent of the presence of S. The quantum yield of these CdSe/CdS particles was 20%, which is similar to the previous CdSe/ZnS results, indicating that CdS shell growth was successful.

To combine the lower lattice strain from CdS with the superior passivation of ZnS, a ZnS shell was overgrown over the CdSe/CdS particles. Particles were synthesized using this method from identical cores using three shell growth methods. One set of particles was created using the standard $ZnDDTC_2$ decomposition at 140 °C. In an alternate procedure to give more time for Zn adsorption, a five minute adsorption step of 110 °C was followed by a $ZnDDTC_2$ decomposition step at 160 °C, similar to a literature method.[23] A third procedure used a S overgrowth step at 220 °C for five minutes followed by the standard 140 °C $ZnDDTC_2$ decomposition step; the S overgrowth was essentially a half-SILAR step meant to promote Zn^{2+} cation adsorption by coating the nanocrystal with a half-monolayer of S. The fluorescence results in Fig. 4 show similar fluorescence for the three shell growth procedures. The CdS/S/ZnS and 110 → 160 °C structures show a modest improvement in QY *versus* the standard procedure (44% *versus* 37% for standard CdSe/CdS/ZnS). Despite passivation, photobleaching did occur over the course of hours when the quantum dots were dispersed on a polymer surface from a hexane solution.[24]

Another goal for these CdSe/CdS/ZnS particles was to achieve longer wavelength emissions in the orange-red region (>590 nm). Longer emission wavelengths were achieved simply by using a longer residence time of 15 minutes for the CdSe/CdS synthesis. Subsequently, ZnS was overgrown using an

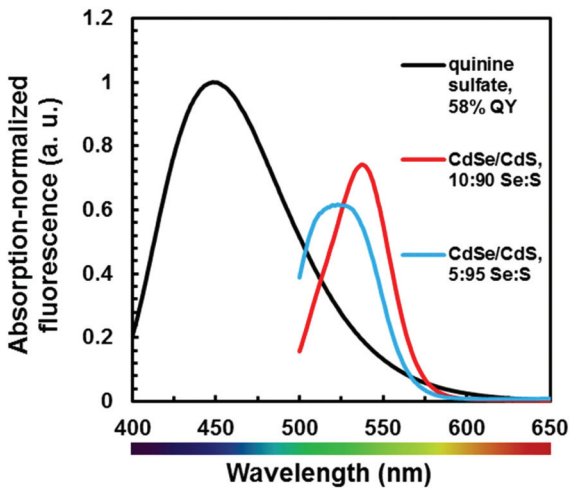

Fig. 3 Absorption-normalized fluorescence for CdSe/CdS particles as a function of Se : S ratio. Excitation: 490 nm. Fluorescence below 500 nm is not shown due to proximity to the excitation signal.

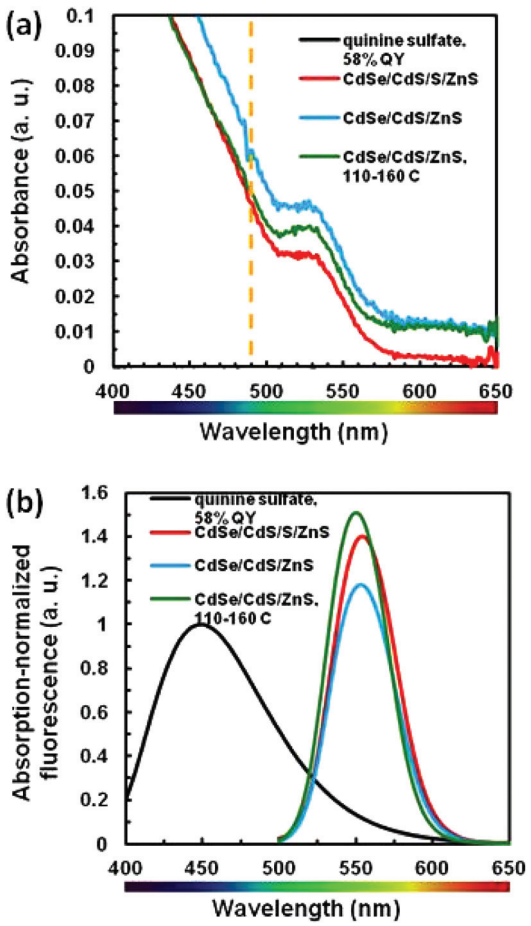

Fig. 4 (a) Absorbance and (b) fluorescence spectra of CdSe/CdS/ZnS quantum dots in arbitrary units with varying shell growth procedure. Excitation: 490 nm.

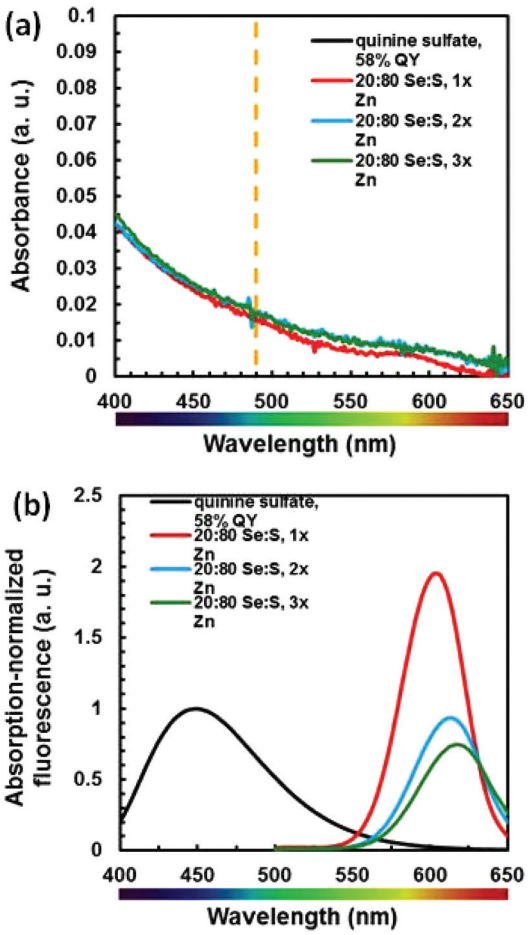

Fig. 5 (a) Absorbance and (b) fluorescence spectra of CdSe/CdS/ZnS quantum dots in arbitrary units with varying ZnS shell growth amount. 1, 2, or 3 additions corresponds to ~2, 4, or 6 monolayers. Excitation: 490 nm.

110 → 140 °C shell growth procedure in ~2 monolayer increments. Fig. 5 shows the absorbance and fluorescence spectra for the CdSe/CdS/ZnS particles, which show orange fluorescence peaks at 604, 614, and 618 nm as more ZnS is grown causing a redshift. The quantum yield decreases sharply from a maximum of 60% with ~2 monolayers (1 addition) to 32%, then 27% with further additions of the $ZnDDTC_2$ precursor. This result is consistent with literature knowledge for CdSe that 1–2 monolayers of ZnS is optimal before lattice strain starts to reduce quantum yield.[6] The FWHM for the particles increased from 48 nm with ~2 monolayers of ZnS to 55 nm with ~6 monolayers of ZnS. These results show that ~2 monolayers of ZnS is optimal for these particles from both a performance and process standpoint.

Synthesis of CdS/ZnS nanoparticles

To achieve shorter wavelength emission, CdS was used in place of CdSe. CdS has a larger band gap which enables purple-blue emission for particles that are much larger than the equivalent emission CdSe particles, allowing for easier synthesis and higher reaction temperatures. Preliminary studies focused on synthesizing CdS/ZnS particles using TOP-S in place of TOP-Se in a procedure otherwise identical to that used for CdSe/ZnS. The initial CdS particles had quantum yield of 17% and FWHM of only 28 nm (Fig. 6), showing that use of the less reactive TOP-S reduces size dispersion relative to use of TOP-Se. The peak was centered at 443 nm, which is near the boundary between purple and blue emission. Unfortunately, ZnS shell growth over these particles almost entirely quenched the fluorescence and caused orange trap emission to be the dominant product (Fig. 6). The fluorescence was greatly reduced, with the new particles producing <1% QY overall. However, small signs of a core–shell peak appeared at 460 nm, consistent with shell growth causing a red shift. Based on this result, a hypothesis was generated that the poor shell growth was due to improper $ZnDDTC_2$ adsorption on the particle surface; partial ZnS overgrowth would disrupt the surface and create sites for traps. To improve $ZnDDTC_2$ adsorption, a core growth procedure was developed that removed the passivating ligand TOP from the reaction mixture. This simplified procedure dissolved the same amount of S in ODE using the term-

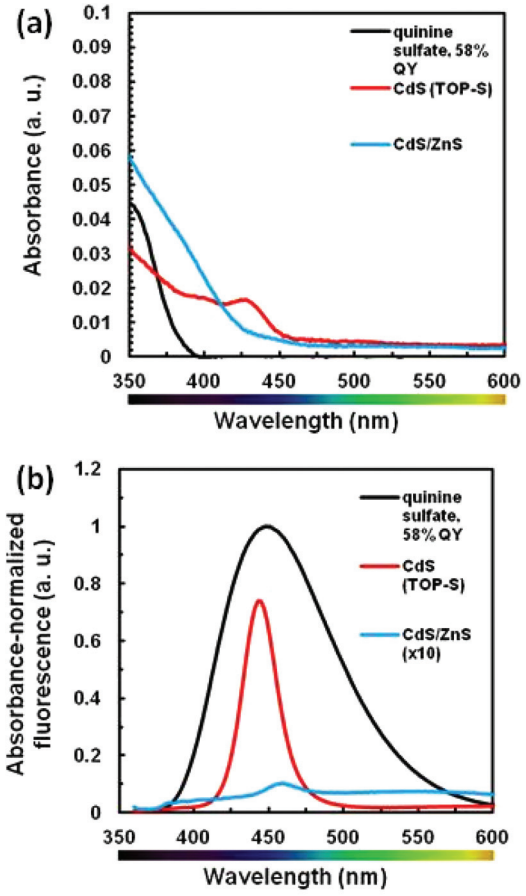

Fig. 6 (a) Absorbance and (b) fluorescence spectra of CdS/ZnS quantum dots in arbitrary units with and without shell growth. CdS/ZnS fluorescence is shown 10 times higher than measured to show the peak location. Excitation: 490 nm.

inal double bond as a ligand to bind S and removed the need to use a glove box with the S binding. The cores produced from this procedure are similar in quality to the CdS cores formed with TOP-S. However, the quantum yield after ZnS overgrowth was much higher than when using TOP-S and yielded minimal trap emission (Fig. 7). A quantum yield of 23% was achieved with a FWHM of 31 nm, which was considerably narrower than the CdSe/ZnS particles. The ZnS added was approximately 2 monolayers; additions to grow the particles to approximately 4 or 6 monolayers decreased quantum yield without significantly changing FWHM or peak location. The purple-blue emission (431 nm) obtained from these particles substantially increases the range of colors possible from the flow reactor, although the quantum yield is not substantially higher than the core particles.

Due to concerns about the low reactivity of the S-rich surface, an alternate core–shell synthesis focused on forming CdS with a small amount of CdSe (9 : 1 ODE-S : TOP-Se ratio) to promote $ZnDDTC_2$ adsorption. This procedure was intended to use the larger band gap of CdS to achieve purple emission while utilizing the higher reactivity of Se to promote ZnS attachment and shell growth. Fig. 8a shows the absorbance at 1/40 concentration for the 10 : 90 Se : S CdSeS particles, which

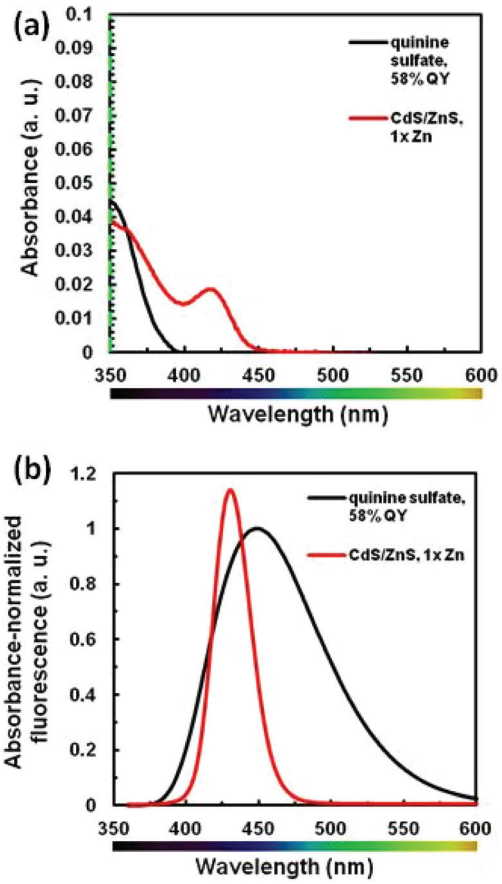

Fig. 7 (a) Absorbance and (b) fluorescence spectra of CdS/ZnS quantum dots in arbitrary units. Excitation: 490 nm.

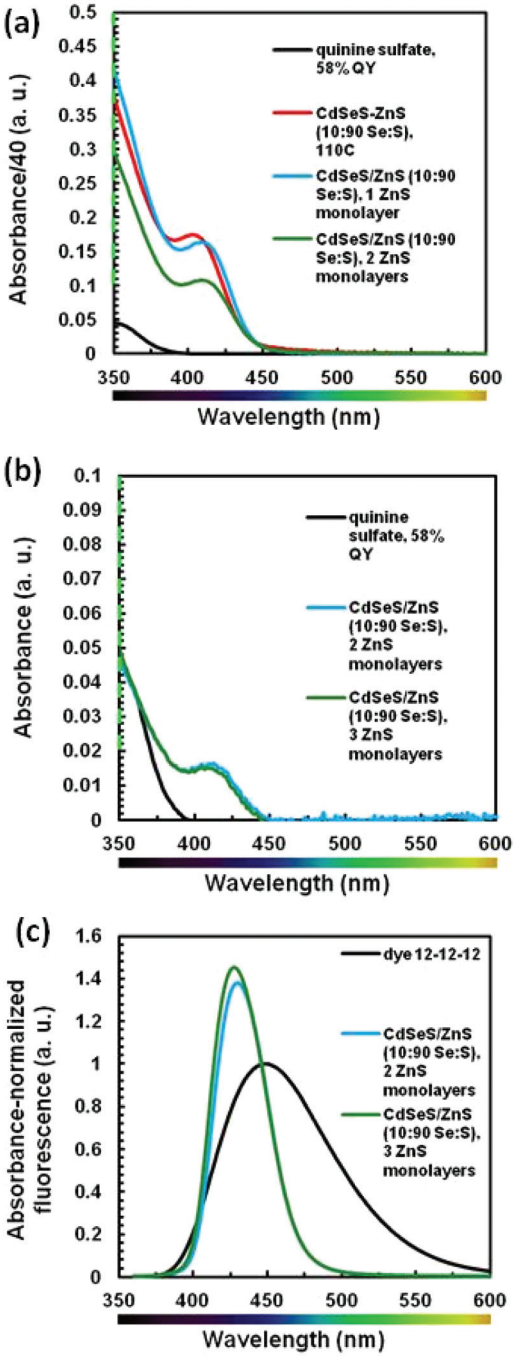

Fig. 8 (a) Absorbance at 1/40 dilution, (b) absorbance in arbitrary units, and (c) absorption-normalized fluorescence in arbitrary units for CdSeS/ZnS particles with varying ZnS monolayers.

have behavior similar to that of the CdS particles. After the absorbance was diluted to obtain absorbance values below 0.1 at 350 nm, in accordance with our standard procedure, the quantum yield of CdSeS/ZnS particles with two monolayers of ZnS was 38% while CdSeS/ZnS particles with three monolayers of ZnS had quantum yield of 40% (Fig. 8c). This result differs from the ZnS shell results for CdSe due to the lower lattice

strain between CdS and ZnS; further ZnS overgrowth did decrease performance possibly due to defect site accumulation.

The higher absorbance of CdSeS and CdS particles can cause higher effective fluorescence output relative to CdSe. Both 10 : 90 Se : S CdSeS and CdS particles have substantially higher absorbance (0.3–0.42) at the excitation wavelength of 350 nm than CdSe particles, which have absorbance around 0.05 at the excitation wavelength of 490 nm. Since fluorescence is proportional to absorbance, the CdSeS and CdS particles in a given volume produce higher total fluorescence relative to CdSe even when considering the higher quantum yield from CdSe particles.

Synthesis of CdSeS/ZnS nanoparticles

CdSeS particles have the ability to generate fluorescence peaks intermediate between CdS and CdSe, making them desirable to target specific wavelengths. To generate alloy nanoparticles, Se and S precursors with similar reactivity are generally required. Although there is literature work showing that TOP-Se : TOP-S ratios of 1 : 7 or lower can yield alloy nanocrystals, this method results in large amounts of excess sulfur, which can interfere with subsequent synthesis steps and leaves excess reactants in the mixture.[25] The large excess of sulfur is required due to the lower reactivity of sulfur as compared to selenium. Here, TOP-Se was combined in a 50 : 50 molar ratio with ODE-S, which is more reactive than TOP-S. The resulting cores showed appropriate alloy behavior intermediate between the CdS and CdSe behavior with a peak location of 483 nm (Fig. 9). CdS particles in this emission range would be considerably larger, reducing their stability in a colloidal mixture, while CdSe particles in this emission range would be very small and difficult to synthesize. Increased residence time to 15–18 minutes resulted in lower quantum yield for the cores (2% for 15–18 minutes *vs.* 5% for three minutes) and a red-shifted peak location of 502 nm. Changing the residence time offers a simple way to tune the peak location, but very large particles would be better replaced by CdSe particles. At 3 minute residence times, the capability for high throughput particle production compares favourably to work focused on high throughput QD production reported in the literature, due to higher flow rates used in our work (5–10 ml min^{-1} of reagent in this system *vs.* 3 ml min^{-1} through five parallel channels) as well as the omission of an overnight aging step post-mixing.[14]

ZnS was overgrown over the CdSeS cores synthesized with a three minute residence time to make CdSeS/ZnS particles with shells of 2, 4, and 6 monolayers (1, 2, or 3 $ZnDDTC_2$ additions of ~2 monolayers each). The resulting quantum yields were 49%, 46%, and 30% respectively, with peak locations in the range of 490–493 nm. These results indicate that growing 4 or more ZnS monolayers decreased the quantum yield; however, this decrease was not as sharp as the decline observed with the 20 : 80 Se : S CdSe/CdS/ZnS particles. This shell growth behavior supports the hypothesis that CdSeS alloy formation occurred, as opposed to small CdSe particles with a CdS shell.

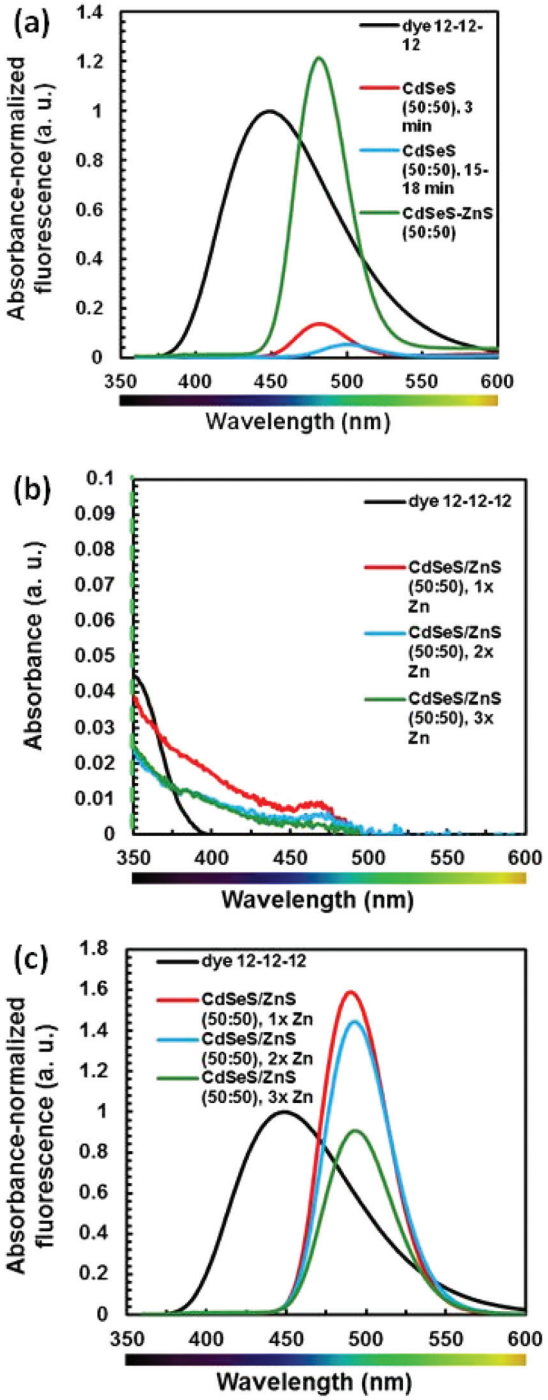

Fig. 9 (a) Absorbance-normalized fluorescence of CdSeS cores, (b) absorbance, and (c) absorbance-normalized fluorescence spectra of CdSe/CdS/ZnS quantum dots in arbitrary units with varying shell growth procedure. Excitation: 490 nm.

The peak location of the CdSeS is also blue-shifted relative to the 20 : 80 CdSe despite the presence of more Se in the CdSeS, which would normally create larger particles and cause a red-shift. Thus, these results demonstrate the successful synthesis of CdSeS/ZnS particles with good quantum yield.

Conclusions

In summary, we reported the liquid phase heat injection synthesis of CdSe, CdS, and CdSeS (alloy) quantum dots in single step procedures that did not require in-line mixing. Quantum yields of up to 60% were achieved by overgrowing ZnS shell or CdS shells with only one added reaction step in the case of CdSe or CdSeS. These syntheses also focused on stoichiometric chemistry, reducing wasted reagents and increasing the viability of solvent recycling. The entire visible spectrum ranging from purple-blue to orange was covered, indicating the versatility of the reactant system, and flow rates were higher (on the order of 10 mL min^{-1}) than comparable flow reactors also used to synthesize quantum dots.

Future work in this area could focus on further improving quantum yield, reducing photobleaching, and reactor throughput. Improved quantum yield is always desirable for fluorescence and could be examined by optimizing shell growth in smaller increments and changing reagent concentration. Reduced photobleaching could be achieved *via* thicker shell growth. Improved throughput could be achieved with higher flow rates while keeping the residence time constant or by scaling out, that is creating multi-channel reactors.

Acknowledgements

We gratefully acknowledge financial support from the Dow Chemical Company for research agreement #226772AC and a graduate fellowship to MSN. We thank Steven Warren for assistance with TEM imaging as well as Dr Pete Trefonas, Dr Jieqian Zhang, Dr Jong Park, You "Andy" Zhai, and Nuri Oh for stimulating discussions.

References

1 D. Bera, L. Qian, T.-K. Tseng and P. H. Holloway, *Materials*, 2010, **3**, 2260–2345.
2 J. L. West and N. J. Halas, *Annu. Rev. Biomed. Eng.*, 2003, **5**, 285–292.
3 H. Yang, W. Luan, Z. Wan, S.-t. Tu, W.-K. Yuan and Z. M. Wang, *Cryst. Growth Des.*, 2009, **9**, 4807–4813.
4 T. Trindade, P. O'Brien and X.-m. Zhang, *Chem. Mater.*, 1997, **9**, 523–530.
5 J. R. Dethlefsen and A. Døssing, *Nano Lett.*, 2011, **11**, 1964–1969.
6 R. Xie, U. Kolb, J. Li, T. Basche and A. Mews, *J. Am. Chem. Soc.*, 2005, **127**, 7480–7488.
7 P. Reiss, J. l. Bleuse and A. Pron, *Nano Lett.*, 2002, **2**, 781–784.
8 P. Laurino, R. Kikkeri and P. H. Seeberger, *Nat. Protocols*, 2011, **6**, 1209–1220.
9 S. G. Kwon and T. Hyeon, *Small*, 2011, **7**, 2685–2702.
10 H. Wang, H. Nakamura, M. Uehara, Y. Yamaguchi, M. Miyazaki and H. Maeda, *Adv. Funct. Mater.*, 2005, **15**, 603–608.
11 J. Pan, A. O. El-Ballouli, L. Rollny, O. Voznyy, V. M. Burlakov, A. Goriely, E. H. Sargent and O. M. Bakr, *ACS Nano*, 2013, **7**, 10158–10166.
12 B. K. H. Yen, A. Günther, M. A. Schmidt, K. F. Jensen and M. G. Bawendi, *Angew. Chem., Int. Ed.*, 2005, **117**, 5583–5587.
13 A. M. Nightingale, S. H. Krishnadasan, D. Berhanu, X. Niu, C. Drury, R. McIntyre, E. Valsami-Jones and J. C. deMello, *Lab Chip*, 2011, **11**, 1221–1227.
14 A. M. Nightingale, J. H. Bannock, S. H. Krishnadasan, F. T. F. O'Mahony, S. A. Haque, J. Sloan, C. Drury, R. McIntyre and J. C. deMello, *J. Mater. Chem. A*, 2013, **1**, 4067.
15 T. W. Phillips, I. G. Lignos, R. M. Maceiczyk, A. J. deMello and J. C. deMello, *Lab Chip*, 2014, **14**, 3172–3180.
16 T. Omata, K. Nose, S. Otsuka-Yao-Matsuo, H. Nakamura and H. Maeda, *Jpn. J. Appl. Phys.*, 2005, **44**, 452.
17 M. Moghaddam, M. Baghbanzadeh, A. Sadeghpour, O. Glatter and C. O. Kappe, *Chem. – Eur. J.*, 2013, **19**, 11629–11636.
18 A. M. Nightingale and J. C. de Mello, *J. Mater. Chem.*, 2010, **20**, 8454.
19 S. Biswas, J. T. Miller, Y. H. Li, K. Nandakumar and C. S. S. R. Kumar, *Small*, 2012, **8**, 688–698.
20 S. E. Lohse, J. R. Eller, S. T. Sivapalan, M. R. Plews and C. J. Murphy, *ACS Nano*, 2013, **7**, 4135–4150.
21 W. W. Yu, L. Qu, W. Guo and X. Peng, *Chem. Mater.*, 2003, **15**, 2854–2860.
22 S. K. Bhunia, A. Saha, A. R. Maity, S. C. Ray and N. R. Jana, *Sci. Rep.*, 2013, 3.
23 D. Chen, F. Zhao, H. Qi, M. Rutherford and X. Peng, *Chem. Mater.*, 2010, **22**, 1437–1444.
24 G. G. See, L. Xu, M. S. Naughton, T. T. Tang, Y. Bonita, J. Joo, P. Trefonas, K. Deshpande, P. J. A. Kenis, R. G. Nuzzo and B. T. Cunningham, *Appl. Opt.*, 2015, **54**, 2302–2308.
25 E. Jang, S. Jun and L. Pu, *Chem. Commun.*, 2003, 2964–2965, DOI: 10.1039/b310853h.